DOI 10.24425/aee.2024.149931

A power shaping based control strategy for dual active full-bridge converter

YAJING ZHANG[1]✉, HAO MA[1], XIUTENG WANG[2], TIANCONG SHAO[3]

[1]*School of Automation, Beijing Information Science and Technology University*
No. 12 Qinghe Xiaoying East Road, Haidian District, Beijing, China

[2]*Branch of Resource and Environment, China National Institute of Standardization*
No. 4 Zhi Chun Road, Haidian District, Beijing, China

[3]*Branch of Resource and Environment, China National Institute of Standardization*
No. 4 Zhi Chun Road, Haidian District, Beijing, China

e-mail: {✉ zhangyajing/2022020463}@bistu.edu.cn, wangxt@cnis.ac.cn, haotc@bjtu.edu.cn

(Received: 18.02.2024, revised: 07.05.2024)

Abstract: Dual active full-bridge (DAB) DC–DC converters are widely used in DC microgrids and various fields of power electronics. It has the advantages of high-power density, easy to implement soft switching and bi-directional power transfer capability. Conventional linear controllers have difficulty in meeting the increasing demands for speed and robustness. In this paper, a control strategy based on the Brayton–Moser theory of power shaping is proposed to improve the control strategy of DAB DC–DC converters. The DAB DC–DC converter is modelled and the controller is designed based on the Brayton–Moser power-shaping theory. A simulation of the DAB DC–DC converter is constructed and a comparative analysis is carried out for three control strategies of PI control, passive control and power-shaping Brayton–Moser control under different operating conditions.

Key words: Brayton–Moser theory, DAB topology, DC microgrids, passive control

1. Introduction

With the development of increasing energy demand, DC–DC converters are widely used in electric vehicle charging and DC microgrids. Among them, bidirectional energy flow, high transmission efficiency, electrical isolation and low reactive power demand are the advantages of dual active bridge (DAB) DC–DC converters, which are widely used in electric vehicles, new energy generation and energy storage [1–3]. However, since the power electronic converter is a highly coupled nonlinear system that can be affected by circuit parameter disturbances, load and

input voltage variations, and unmodeled dynamics, the use of traditional linear control methods can no longer meet the requirements of high-performance systems in practical applications.

As more and more scholars at domestic and abroad have carried out research on the DAB DC–DC converter, it has also been widely used in practical engineering. Xia *et al*. [4] proposed a quasi-single stage DC–DC converter integrating the dual active bridge (DAB) and buck-boost (IDABBB) for wide output voltage range applications, which has excellent performances in terms of efficiency, cost, and power density. Chen *et al*. [5] put forward a power balance control based on return power optimization for the DAB converter, which ensures good power balance, evidently reduces the return power and improves the dynamic response of the system. Siddhant Bikram Pandey *et al*. [6] proposed a hybrid modulation scheme using single-phase shift (SPS) and dual-phase shift (DPS) control for on-board charger (OBC) applications requiring high power and a wide voltage range to reduce the rms currents and conduction losses at higher voltage levels and to achieve zero-voltage for all the switches over a wide range of battery zero-voltages switching (ZVS) turn-on. Mridul Mishra *et al*. [7] analyzed the operation of a DAB DC–DC converter in constant-current (CC) and constant-voltage (CV) operating modes for electric vehicle battery charging applications. Scholars have proposed many nonlinear control methods for DAB DC–DC converters.

In recent years, nonlinear control algorithms have attracted much attention in the field of power electronics, such as sliding mode control [8], non-smooth control [9], passive control [10], model predictive control [11] and adaptive control [12]. The above nonlinear control has many limitations, such as having a relative order limitation, as well as low control accuracy, complex calculations, and lower generalizability, among others, and needs further improvement. Among them, nonlinear control based on passive ideas is widely used by researchers, it has the advantages of no overshoot, high stability and good robustness [13–15], is very suitable for application in the field of complex industrial control where there are fluctuations in parameters. Meanwhile, compared with many nonlinear control strategies, the algorithmic logic structure of passive control is simple and easy to program and implement, so it has attracted much attention.

The basic theory of passive control was proposed in the 1950s by two scholars, Lurie and Popov, who linked its concept with stability and applied it to control strategy, and then gradually developed into the current passive theory through the in-depth study of scholars such as Yakubovich, Hill and Moylan [16]. The essence of passive controller design is to control the energy distribution of the system, the basic idea of the design is: first of all, the “reactive term” of the system is separated from the system, because the “reactive term” does not affect the energy of the system and will not destabilize the system, so it can be conFigured arbitrarily [17]. The appropriate conFiguration of the "reactive term" in the system is done by adding damping to the system, so that the total energy function of the system follows the given energy function, the closed loop system is passive, and the system is guaranteed to be stable, so that the state variables of the controlled system do not differ from the reference values of the given state variables. Passive control shifts the research framework of control theory from the traditional signal processing perspective to the energy processing (transmission) perspective, and its physical concepts are very intuitive and easy to be accepted by engineers, and there exist a wide range of applications in many practical physical systems. The core of it is to start from the energy point of view so that the closed-loop system satisfies passivity. The error between the state variables of the controlled system and the reference value of the given state variables converges asymptotically to zero [18].

At present, there are two common forms of passive controller design, one is to establish the Euler-Lagrange (EL) model of the system and perform the passive controller design by damping injection. The other one is to establish the Port Controlled Hamilton (PCH) model of the system and perform the passive controller design by the Interconnection and Damping Assignment Passivity Based Control (IDA-PBC) method. The more mature application of these two controller design methods is the EL-based system passive controller, which has been successfully applied to a variety of power electronic converters such as PWM rectifiers, multi-level rectifiers, DC/DC converters, UPS converters, multi-level inverters, active power filters, etc. The design of this control method has been successfully applied to a variety of power electronic converters. Reference [19] proposed the Brayton–Moser (BM) control method based on the passive theory, from the perspective of the system instantaneous power can be converter voltage and current and other variables can be directly introduced into the model, and has no overshoot, high stability, fast response speed, robustness and other advantages [20].

In this regard, scholars at domestic and abroad have used the theory of the Mixed Potential Function (MPF) to analyze the stability and stability conditions of the system based on the Brayton–Moser (BM) model, and have obtained good results. Kumari SHIPRA *et al*. [21] developed a dynamic model of a three-stage boost converter using the BM theory and completed the control strategy based on the BM theory by injecting virtual resistors. Tomoaki Hashimoto [22] investigated the predictive control model using the discrete BM theory and proposed a prediction method for discrete-time nonlinear systems and provided a numerical solution based on the C/GMRES algorithm to solve the prediction problems. Sonal Gedam *et al*. [23] used the power of the system to construct a model and proposed the use of the BM theory as a new building block for modelling and analysis of switching systems. The theory is also demonstrated using the example of a solid-state transformer (SST). This control strategy is used to design the controller for the system from the perspective of system energy, and has been applied in several research areas in recent years, such as electric vehicles and power systems [24, 25]. Based on this, the BM theory has gradually gained rapid development by improving the stability of control and enhancing the dynamic response in both energy-shaping and power-shaping.

The Brayton–Moser theory allows a dynamic system to be studied in terms of its stability and dynamic performance by means of directly observable quantities, organizing the dynamic equations of the circuit into the form of the Brayton–Moser model including the terms of its derivative of the power mixing potential function and the other term containing the duty cycle. In the mixed potential function, in order to satisfy the power balance inequality, the matrix Q which contains the dynamic original elements the inductance and the capacitor, needs to satisfy the negative definiteness, so that new P and Q are constructed to maintain the stability of the system. The new circuit system after the equivalence satisfies the conditions for the BM model to hold, so the controller is designed on this basis and the duty cycle is obtained to finally achieve the stability of the DAB controller. The stability of the BM method is verified by applying the second method of the Lyapunov stability in the theoretical part, and its stability, robustness and good dynamic performance are verified in the simulation part.

This paper is divided into the following sections: Section 1 gives the development history of passive control and the current status of domestic and international research on the BM theory, and presents the research content of this paper. In Section 2, the BM theory [26] based on power shaping is briefly introduced. Based on the topology, the mathematical model of the DAB DC–DC

converter is given and the stability analysis is carried out. In Section 3, the controller based on the power shaping BM theory is designed. In Section 4, a simulation of the DAB DC–DC converter is constructed and the effectiveness of the BM control strategy is demonstrated by comparing with the PI control strategy and passive control under different operating conditions. Finally, the conclusions of this study are presented in Section 5.

In this paper, the control strategy of the DAB converter is further investigated. The main contributions of this paper include:

1. For the first time, a DAB DC–DC converter control strategy based on the BM theory in the form of power shaping is proposed, and a more detailed discussion, mathematical model and formulas are given.
2. By the proposed strategy, multiple dynamic responses of the DAB DC–DC converter based on the BM theory control method are achieved.
3. The BM control strategy has been improved effectively under various operating conditions compared with PI control and passive control.

2. Brayton–Moser model based on power shaping

As shown in Fig. 1, the topology of the dual active full-bridge DC–DC converter consists of a full-bridge converter on the primary side, a high-frequency transformer (HFT) and a full-bridge converter on the secondary side. The full-bridge converter realizes DC–AC, AC–DC voltage conversion, while the high-frequency transformer can realize the voltage matching between the primary side and the secondary side, electrical isolation, as well as the temporary storage of energy.

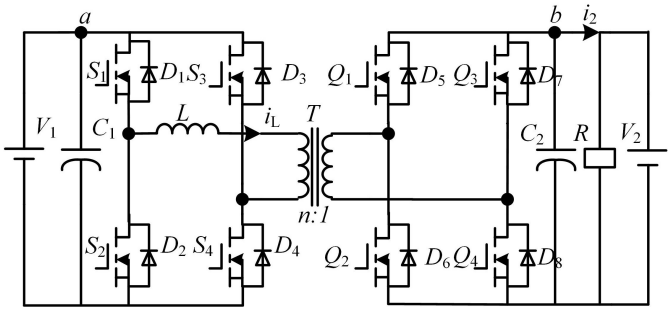

Fig. 1. The topology of dual active full bridge DC–DC converter

In Fig. 1, we used SPS (Single-phase-shift) modulation, the primary-side full-bridge converter consists of four MOSFETs ($S_1 - S_4$) and filter capacitors C_1.The secondary-side full-bridge converter is similar to the primary-side full-bridge converter and consists of four MOSFETs ($Q_1 - Q_4$) and filter capacitors C_2. Due to the similarity of the primary-side and secondary-side operating mechanisms, the MOSFET S_1 and S_4 turn on complementary to each other, and the MOSFET S_2 and S_3 turn on at the same time, generating square wave voltages V_{H1} and V_{H2} with a 50% duty cycle on the primary and secondary sides of the transformer T. V_1 is the input voltage, V_1 is the output voltage. i_L is the average value inductance current and n is the transformer ratio.

The dynamic model of the DAB converter based of the Brayton–Moser theory is:

$$\begin{cases} L\dfrac{\mathrm{d}i_L}{\mathrm{d}t} = V_1 - nV_2 \\ C_2\dfrac{\mathrm{d}V_2}{\mathrm{d}t} = \dfrac{nV_1}{2f_sL}d(1-d) - \dfrac{V_2}{R} \end{cases}. \tag{1}$$

Among them, L is the inductance of the circuit, C_2 is the filter capacitors, and i_L represents the average value of inductive current, V_2 is the output voltage on the secondary side. We introduce the drive amount D, and there exists $D = d(1-d)$, where $X = [i_L V_2]^T = [x_1 x_2]^T$ is substituted into the above model. Then we obtain:

$$\begin{cases} -L\dfrac{\mathrm{d}i_L}{\mathrm{d}t} = nV_2 - V_1 \\ C_2\dfrac{\mathrm{d}V_2}{\mathrm{d}t} = \dfrac{nV_1}{2f_sL}D - \dfrac{V_2}{R} \end{cases}. \tag{2}$$

To facilitate the design of the controller, the compact form of the BM model of the nonlinear system is denoted as:

$$\boldsymbol{Q}\dot{x} = \frac{\partial \boldsymbol{P}(\boldsymbol{x})}{\partial \boldsymbol{x}} - \hat{\boldsymbol{B}}\boldsymbol{u}. \tag{3}$$

The matrix $\boldsymbol{Q} = \mathrm{diag}\{-L, C_2\}$ is the matrix which consists of the inductance L and the filter capacitors C_2,

$$\boldsymbol{X} = [x_1 x_2]^T, \quad \frac{\partial \boldsymbol{P}(\boldsymbol{x})}{\partial \boldsymbol{x}} = \begin{bmatrix} -nV_2 + V_1 \\ -\dfrac{V_2}{R} \end{bmatrix}$$

is the derivative of the mixed potential function, and

$$\hat{\boldsymbol{B}} = \begin{bmatrix} 0 & \\ & -D \end{bmatrix}, \quad \boldsymbol{u} = \begin{bmatrix} 0 \\ \dfrac{nV_1}{2f_sL} \end{bmatrix}.$$

For stability analysis, multiplying $\dot{x}^T$ at both sides of Eq. (3) gives:

$$\dot{x}^T\boldsymbol{Q}\dot{x} = \dot{x}^T\frac{\partial \boldsymbol{P}(\boldsymbol{x})}{\partial \boldsymbol{x}} - \dot{x}^T\hat{\boldsymbol{B}}\boldsymbol{u}. \tag{4}$$

Due to

$$\dot{x}^T\frac{\partial \boldsymbol{P}(\boldsymbol{x})}{\partial \boldsymbol{x}} = \frac{\partial \boldsymbol{P}(\boldsymbol{x})}{\partial \boldsymbol{t}},$$

the condition

$$\frac{\mathrm{d}\boldsymbol{P}(\boldsymbol{x})}{\mathrm{d}\boldsymbol{t}} = \dot{x}^T\boldsymbol{Q}\dot{x} + \dot{x}^T\hat{\boldsymbol{B}}\boldsymbol{u}$$

is satisfied.

Since $\boldsymbol{Q}$ is not a negative-definite matrix, the power balance inequality

$$\frac{\partial \boldsymbol{P}(\boldsymbol{x})}{\partial \boldsymbol{t}} \leq \dot{x}\hat{\boldsymbol{B}}\boldsymbol{u}$$

is not satisfied.

Then the stability of the DAB converter system cannot be ensured. To keep the stability of the DAB converter, a new BM model needs to construct as well as find a new $\widetilde{\boldsymbol{P}}$ and $\widetilde{\boldsymbol{Q}}$. For a given ($\boldsymbol{QP}$) and an arbitrary λ and symmetric matrix $\mathbf{M}$ are chosen:

$$\begin{cases} \widetilde{\boldsymbol{Q}} = \lambda \boldsymbol{Q} + \dfrac{\partial \boldsymbol{P}(\boldsymbol{x})}{\partial \boldsymbol{x}} \boldsymbol{M} \boldsymbol{Q} \left(\dfrac{\partial \boldsymbol{P}(\boldsymbol{x})}{\partial \boldsymbol{x}} \right)^T \\ \hat{\boldsymbol{P}} = \lambda \boldsymbol{P} + \dfrac{1}{2} \left(\dfrac{\partial \boldsymbol{P}(\boldsymbol{x})}{\partial \boldsymbol{x}} \right)^T \boldsymbol{M} \dfrac{\partial \boldsymbol{P}(\boldsymbol{x})}{\partial \boldsymbol{x}} \end{cases}. \tag{5}$$

Thus, the BM model is transformed into: $\widetilde{\boldsymbol{Q}} \dot{x} = \dfrac{\partial \widetilde{\boldsymbol{P}}(\boldsymbol{x})}{\partial \boldsymbol{x}} - \widetilde{\hat{\boldsymbol{B}}} \boldsymbol{u}$, where $\widetilde{\boldsymbol{B}} = \widetilde{\boldsymbol{Q}} \boldsymbol{Q}^{-1} \boldsymbol{B}$.

When the matrix $\widetilde{\boldsymbol{Q}}$ satisfies the negative-definite condition

$$\widetilde{\boldsymbol{Q}}(\boldsymbol{x}) + \widetilde{\boldsymbol{Q}}^{\boldsymbol{T}}(\boldsymbol{x}) \leq 0,$$

there exists

$$\frac{\partial \widetilde{\boldsymbol{P}}(\boldsymbol{x})}{\partial \boldsymbol{t}} \leq \dot{x} \widetilde{\hat{\boldsymbol{B}}} \boldsymbol{u},$$

the system satisfies the power balance inequality condition

$$\widetilde{\boldsymbol{P}}(x(t)) - \widetilde{\boldsymbol{P}}(x(0) \leq \int_0^t u^T(\tau) \widetilde{y}(\tau) \mathrm{d}\tau,$$

where $u^T(\tau)$ is the input and $\widetilde{y}(\tau) = \widetilde{\boldsymbol{B}}^{\boldsymbol{T}} \dot{x}$ is the output under the BM model.

Select

$$\boldsymbol{M} = \begin{bmatrix} -\dfrac{1}{L} & \\ & \dfrac{1}{C_2} \end{bmatrix}, \quad \therefore \widetilde{\boldsymbol{Q}} = \lambda \boldsymbol{Q} + \frac{\partial \boldsymbol{P}(\boldsymbol{x})}{\partial \boldsymbol{x}} \boldsymbol{M} \boldsymbol{Q} \left(\frac{\partial \boldsymbol{P}(\boldsymbol{x})}{\partial \boldsymbol{x}} \right)^T = \begin{bmatrix} -\lambda L & \\ & \lambda C_2 + \dfrac{1}{R} \end{bmatrix},$$

then

$$P(x) = (1 - i_L) n V_2 + V_1 i_L - \frac{1}{2R} V_2^2,$$

there is

$$\therefore \widetilde{\boldsymbol{P}}(x) = -\frac{1}{2L}(V_1 - n V_2)^2 + \frac{1}{2C_2} \cdot \frac{V_2^2}{R^2} - \lambda n V_2 (1 - i_L) - \frac{\lambda}{2R} V_2^2 + \lambda V_1 i_L.$$

We assume that $\widetilde{\boldsymbol{Q}}$ is a negative-definite matrix, we must ensure that the odd-order principal sub-equation is less than 0 and the even-order principal sub-equation is greater than 0. We have

$$\begin{cases} -\lambda L < 0 \\ -\lambda L \left(\lambda C_2 + \dfrac{1}{R} \right) > 0 \end{cases}, \quad \lambda C_2 - \frac{1}{R} < 0.$$

The new BM model is obtained finally as shown in Eq. (6):

$$\begin{bmatrix} -\lambda L & \\ & \lambda C_2 + \dfrac{1}{R} \end{bmatrix} \begin{bmatrix} \dot{i}_L \\ \dot{V}_2 \end{bmatrix} = \begin{bmatrix} \lambda(V_1 + nV_2) \\ \dfrac{n}{L}(V_1 - nV_2) + \dfrac{1}{C_2R^2}V_2 - \lambda n(1 - i_L) - \dfrac{\lambda}{R}V_2 \end{bmatrix} - \begin{bmatrix} 0 & 0 \\ 0 & -D \cdot C_2\left(\lambda C_2 + \dfrac{1}{R}\right) \end{bmatrix} \begin{bmatrix} 0 \\ \dfrac{nV_1}{2f_sL} \end{bmatrix}. \tag{6}$$

3. Controller design based on BM model for power shaping

3.1. Controller design based on BM model of DAB converter

To enhance the dynamic regulation capability of the DAB DC–DC converter to control the voltage, a new potential function $P_d(x)$ needs to be constructed so as to obtain a new closed-loop system $\widetilde{\boldsymbol{Q}}(x)\dot{x} = \nabla P_d(x)$. The equilibrium of the new potential function $P_d(x)$ at the desired value x^* satisfies the condition

$$\begin{cases} \dfrac{\partial \widetilde{\boldsymbol{P}}(\boldsymbol{x})}{\partial \boldsymbol{x}} \mid x = x^* = 0 \\ \dfrac{\partial^2 \widetilde{\boldsymbol{P}}(\boldsymbol{x})}{\partial \boldsymbol{x}^2} \mid x = x^* > 0 \end{cases},$$

where $\boldsymbol{x}^* = [x_1^*, x_2^*]^T = [i_L^*, V_2^*]^T$.

Set the new potential function as $P_d(x) = P(x) + P_a(x)$, we get:

$$\frac{\partial \boldsymbol{P}(\boldsymbol{x})}{\partial \boldsymbol{x}} \Bigg| x = x^* = \begin{bmatrix} \lambda(V_1 + nV_2^*) + \dfrac{\partial P_a(x)}{\partial x} \mid x = x^* \\ \dfrac{n}{L}(V_1 - nV_2^*) + \dfrac{1}{C_2R^2}V_2^* - \lambda n(1 - i_L^*) - \dfrac{\lambda}{R}V_2^* + \dfrac{\partial P_a(x)}{\partial x} \mid x = x^* \end{bmatrix} = 0. \tag{7}$$

Let

$$P_a(x) = \frac{1}{2}k_1(x_1 - x_1^*)^2 + \frac{1}{2}k_2(x_2 - x_2^*)^2 - \frac{1}{L}x_2x_2^*.$$

$P_d(x)$ satisfies the second condition at the desired value of the equilibrium point x^*, it is denoted as:

$$\begin{aligned} P_d(x) = P(x) + P_a(x) = {} & \lambda V_1 i_L - 2\lambda n V_2 i_L + \frac{n}{L}V_1V_2 - \frac{n^2}{2L}V_2^2 + \frac{1}{2C_2R^2}V_2^2 \\ & - \frac{\lambda}{2R}V_2^2 - \frac{1}{L}x_2x_2^* + \frac{1}{2}k_1(x_1 - x_1^*)^2 + \frac{1}{2}k_2(x_2 - x_2^*)^2. \end{aligned} \tag{8}$$

Since the closed-loop system satisfies the condition

$$\widetilde{\boldsymbol{B}}\boldsymbol{u} = \frac{\partial \boldsymbol{P_a}(\boldsymbol{x})}{\partial \boldsymbol{x}},$$

at the equilibrium point there are:

$$\begin{bmatrix} 0 & 0 \\ 0 & -D \cdot C_2(\lambda C_2 + \dfrac{1}{R}) \end{bmatrix} \begin{bmatrix} 0 \\ \dfrac{nV_1}{2f_sL} \end{bmatrix} = \begin{bmatrix} k_1(x_1 - x_1^*) \\ k_2(x_2 - x_2^*) - \dfrac{1}{L}x_2^* \end{bmatrix}. \tag{9}$$

Eventually, the duty cycle is found to be:

$$\begin{cases} d_1 = \dfrac{1}{2} + \dfrac{\sqrt{1 + 4 \cdot \dfrac{k_2(x_2 - x_2^*) - \dfrac{1}{L}x_2^*}{-C_2(\lambda C_2 + \dfrac{1}{R})\dfrac{nV_1}{2f_sL}}}}{2} \\ d_2 = \dfrac{1}{2} - \dfrac{\sqrt{1 + 4 \cdot \dfrac{k_2(x_2 - x_2^*) - \dfrac{1}{L}x_2^*}{-C_2(\lambda C_2 + \dfrac{1}{R})\dfrac{nV_1}{2f_sL}}}}{2} \end{cases}. \tag{10}$$

3.2. Stability analysis of DAB DC–DC converter based on BM model

Figure 2 shows the diagram of BM-based power shaping control strategy for the DAB. To validate the stability of the BM control strategy, the stability of the BM model is obtained by plotting its maximum Lyapunov exponent.

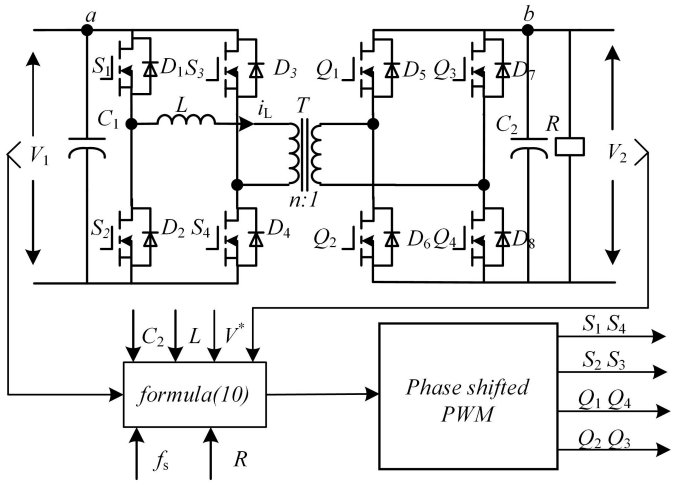

Fig. 2. Diagram of BM power shaping control strategy for DAB

The maximum Lyapunov exponent map based on the Brayton–Moser model is given in Fig. 3. As shown in Fig. 3, it gives the relationships between the Lyapunov exponent LEs and the duty cycle b. The Lyapunov exponent represents the numerical characteristic of the average

exponential divergence rate of adjacent trajectories in phase space. It is found that the maximum Lyapunov exponent is consistently less than 0 which validate the stability of the system. Therefore, the stability of this control strategy is proved.

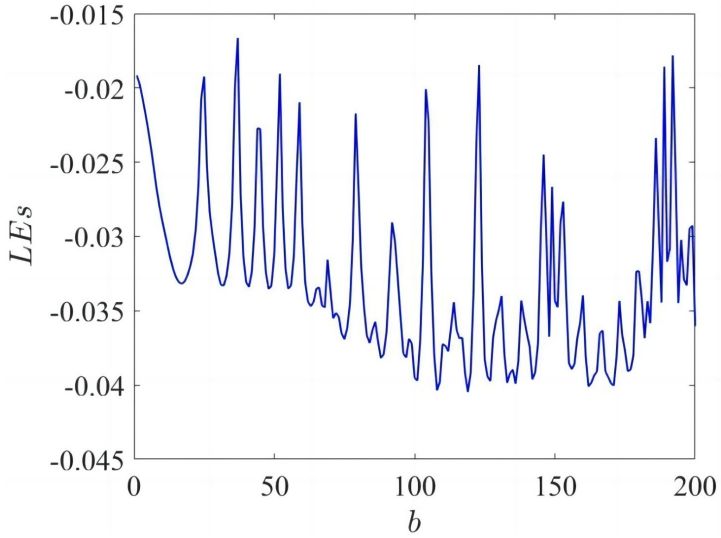

Fig. 3. Maximum Lyapunov exponent map based on BM model

4. Simulation analysis of power shaping based control strategy for DAB converter

To verify the feasibility of the BM control method proposed in this paper, we utilized some power electronics devices of Matlab/Simulink to verify the controller simulation of the DAB converter based on BM-PBC parallel damping, the simulation parameters are shown in Table 1.

Table 1. System simulation parameters

Parameters	**Numerical value**
Input voltage V_1/V	400
Output voltage V_2/V	750
Inductance $L/\mu H$	60
Switching frequency f/kHz	50
Primary side full bridge capacitor C_1/mF	0.7
Sub-side side full bridge capacitor C_2/mF	0.35
Transformer ratio n	1:1

According to parameter values given in Table 1, we compare and analyze BM control compared with EL control and PI control in the DAB converter for the simulation results at the startup phase, the change of desired voltage and the change of bus voltage.

4.1. Stability analysis of DAB DC–DC converter based on BM model

A. Start-up phase simulation

As shown in Fig. 4, the comparison of the start-up phase simulation of the DAB DC–DC converter is given. We tentatively set the output voltage V_2 to be 750 V, and the coefficient of a new BM controller parameter λ is set to be 400, k_1 is 5.11. The proportionality coefficient of PI controller $K_p = 0.0008$, at the same time the integration coefficient $K_i = 0.05$, respectively. Simulation results show that the static effects of all three control strategies are eventually stabilised at 750 V while the speed and the overshoot are different. With BM control, the voltage reaches the desired value in 0.109 s and gradually stabilizes at 750 V. In contrast, the voltage reaches steady state at 0.111 s with EL control, and with PI control, the voltage reaches the desired value at 0.13 s and there is a steady state. The solid yellow line represents PI control, which can be seen in Fig. 4 to have a significant overshoot of 20.6% compared to EL and BM controls. Comparing the three control strategies, the response of the system under BM control and passive control is faster and there is no overshoot under BM control. Compared to EL control, the response speed of BM control is better, which proves that BM control can solve the contradiction between speed and overshoot in PI control more effectively than traditional passive control.

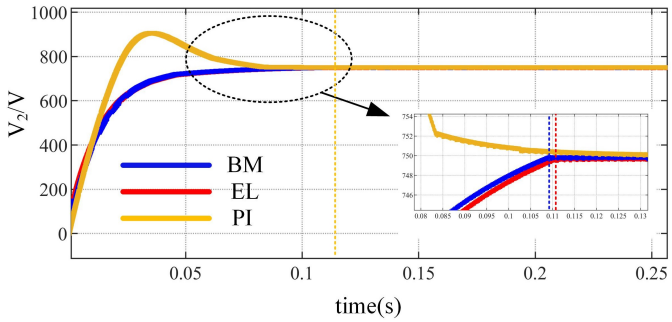

Fig. 4. Comparison of startup phase characteristics simulation of Brayton–Moser control, EL control and PI control

B. Simulation of desired voltage change

The simulated waveform of the current and voltage of the DAB converter when the desired voltage changes is performed as shown in Fig. 5. Firstly, we compare the three control strategies stabilizing at a rate of 650 V when the desired voltage changes. The desired output voltage changes from 750 V to 650 V in 0.2 s, and when the system is controlled by the BM control strategy, it returns to a steady state in 0.2232 s and there is no apparent fluctuation. With EL control, the system returns to a steady state at 0.2402 s, and with PI control, the system reaches a steady state at 0.266 s with a little overshoot, the amount of overshoot is about 1.62%. Comparing the waveforms of the three control strategies, BM control and EL control have a certain degree of speed after

disturbance without obvious fluctuations compared to PI control. From the simulation results, it is concluded that BM control has the better robustness and anti- interference and the fastest stabilization rate when the desired voltage changes abruptly.

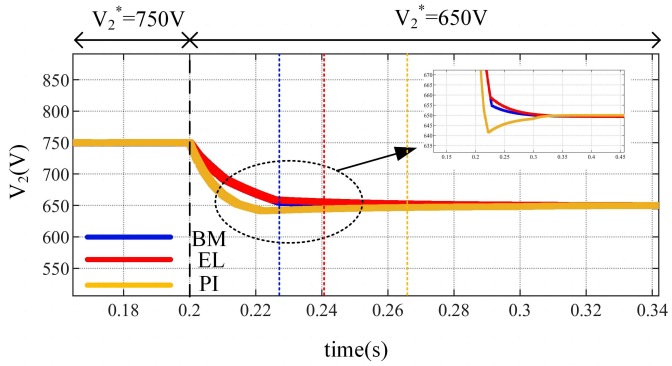

Fig. 5. Comparison of desired voltage change simulation of Brayton–Moser control, EL control and PI control

C. Simulation of bus voltage change

As shown in Fig. 6, the waveform simulation of the current and voltage of the DAB converter during the change of the bus voltage is given, the input voltage changes from 500 V to 400 V in 0.2 s, when the system is controlled with BM control. It returns to a steady state in 0.218 s after the disturbance is added and the voltage stabilizes at 750 V without any obvious fluctuation. The system returns to a steady state in 0.222 s with passive control and in 0.282 s with the PI control. Comparing the waveform of the three control methods, BM control and passive control have more obvious rapidity and less fluctuation after perturbation compare to PI control. At the same time, BM control have better robustness than traditional passive control, the speed of reaching a steady state is faster.

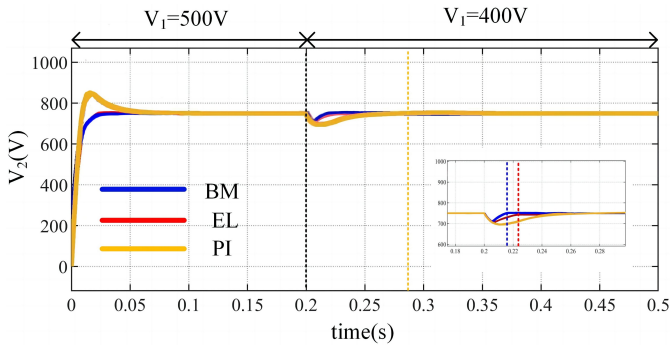

Fig. 6. Comparison of bus voltage change simulation of Brayton–Moser control, EL control and PI control

5. Conclusion

In this paper, the BM control strategy based on power-shaping is proposed, and a nonlinear controller is modelled and designed for the DAB DC–DC converter.

1. Compared with passive control, the proposed control method can more effectively solve the contradiction between overshoot and rapidity in the PI controller.
2. BM control has stronger anti-interference ability and faster speed than passive control in three working conditions: the start-up phase, desired voltage change and bus voltage change.
3. The parameters of the BM control strategy satisfy many different working conditions, the difficulty of the PI control parameter setting has been effectively improved.

Acknowledgements

Project Supported by National Natural Science Foundation of China (52237008, 52107176, 51777012) and the Delta Power Electronics Science and Education Development Program of Delta Group under Grant DREG2022008.

References

[1] Tao L., Yang X., Yang X., Peng X., Yang L., Lang H., Xiang H., *Adaptive voltage control scheme for DAB based modular cascaded SST in PV application*, 2018 International Power Electronics Conference (IPEC-Niigata 2018 ECCE Asia), pp. 1478–1483 (2018), DOI: 10.23919/IPEC.2018.8507808.

[2] Shuyu C., Sriram V.B., Tafti H.D., Ravi Kishore K.V., *Modular DAB DC–DC converter low voltage side dc link capacitor two-stage charging-up control for solid state transformer application*, 2017 AsianConference on Energy, Power and Transportation Electrification (ACEPT), pp. 1–7 (2017), DOI: 10.1109/ACEPT.2017.8168624.

[3] Saha J., Subramanium A., Panda S.K., *Design of Integrated Medium Frequency Transformer (iMFT) for Dual-Active-Bridge (DAB) Based Solid-State-Transformers*, 2021 IEEE 12th Energy Conversion Congress and Exposition-Asia (ECCE-Asia), pp. 893–898 (2021), DOI: 10.1109/ECCE-Asia49820.2021.9479113.

[4] Yuhan X., Xin Z., Qingxin T., Xuwei D., Zhaoyang X., *Quasi-Single Stage DC–DC Converter Integrating DAB and Buck-Boost for Wide Output Voltage Range Applications*, 2023 IEEE 18th Conference on Industrial Electronics and Applications (ICIEA) (2023), DOI: 10.1109/ICIEA58696.2023.10241460.

[5] Zhihao C., Zhenbin Z., Xiaozhe S., Zhen L., Xiaozhe L., *An Optimized Return Power Control for DAB Converter Cluster with ISOP ConFiguration*, 2023 IEEE 2nd International Power Electronics and Application Symposium (PEAS) (2023), DOI: 10.1109/PEAS58692.2023.10395051.

[6] Siddhant Bikram P., Tat-Thang L., Sunju K., Tuan Nguyen M., Sewan C., *Analysis and Implementation of a DAB DC–DC Converter for OBC Application with Wide Output Voltage Range*, 2023 11th International Conference on Power Electronics and ECCE Asia (ICPE 2023 – ECCE Asia) (2023), DOI: 10.23919/ICPE2023-ECCEAsia54778.2023.10213911.

[7] Mridul M., Indrajit S., *EV Battery Charging using DAB DC–DC Converter with EPS and DPS modulations*, 2023 IEEE International Students' Conference on Electrical, Electronics and Computer Science (SCEECS) (2023), DOI: 10.1109/SCEECS57921.2023.10063090.

[8] Pengchao H., Xingcheng W., Yang S., *Research on Flux-Weakening Control System of Interior Permanent Magnet Synchronous Motor Based on Fuzzy Sliding Mode Control*, 2019 Chinese Control and Decision Conference (CCDC), pp. 3151–3156 (2019), DOI: 10.1109/CCDC.2019.8832483.

[9] Zhipeng D., Jiamei J., Liang W., *Adaptive Inverse Control of Piezoelectric Actuator with non-Smooth Hysteresis Model*, 2022 16th Symposium on Piezoelectricity, Acoustic Waves, and Device Applications (SPAWDA), pp. 401–407 (2022), DOI: 10.1109/SPAWDA56268.2022.10046038.

[10] Xiaobin M., Jiuhe W., Weimin W., *A modified multifrequency passivity-based control for shunt active power filter with model-parameter-adaptive capability*, IEEE Transactions on Industrial Electronics, vol. 65, no. 11, pp. 70–769 (2018), DOI: 10.1109/TIE.2017.2733428.

[11] Suleman S., Wenxiang Z., Huanan W., *Fault-tolerant deadbeat model predictive current control for a five-phase PMSM with improved SVPWM*, Chinese Journal of Electrical Engineering, vol. 7, no. 3, pp. 111–123 (2021), DOI: 10.23919/CJEE.2021.000030.

[12] Javier Blanco R., Basil Mohammed A., Roberto Gonzalez H., *Speed control of a magnetic accelerator using adaptive control techniques*, IEEE Latin America Transactions, vol. 20, no. 3, pp. 488–495 (2022), DOI: 10.1109/TLA.2022.9667148.

[13] Ortega R., van der Shaft A., Bernhard M., Escobar G., *Interconnection and damping assignment passivity-based control of port controlled Hamiltonian systems*, Automatica, vol. 38, pp. 585–596 (2002).

[14] Xin L., Xiaodong F., *Passive Backstepping Control of Dual Active Bridge Converter in Modular Three-Port DC Converter*, Electronics, vol. 12, no. 5, pp. 1–11 (2023), DOI: 10.3390/electronics12051074.

[15] Marco C., Sriram J.K., Siddharth K.B., *Port Controlled Hamiltonian Modeling and IDA-PBC Control of Dual Active Bridge Converters for DC Microgrids*, IEEE Transactions on Industrial Electronics, vol. 66, no. 11, pp. 9065–9075 (2019), DOI: 10.1109/TIE.2019.2901645.

[16] Escobar G., Chevreau D., Ortega R., Mendes E., *An Adaptive Passivity-Based Controller for a Unity Power Factor Rectifier*, IEEE Transactions on Control Systems Technology, vol. 9, no. 4, pp. 637–644 (2001), DOI: 10.1109/87.930975.

[17] Xin C., Yang Z., Shanshan W., Jie C., Chunying G., *Impedance-Phased Dynamic Control Method for Grid-Connected Inverters in a Weak Grid*, IEEE Transactions on Power Electronics, vol. 32, no. 1, pp. 274–2834 (2017), DOI: 10.1109/TPEL.2016.2533563.

[18] Rafael C., Fernando Mancilla D., Romeo O., *Passivity-Based Control of a Grid- Connected Small-Scale Windmill with Limited Control Authority*, IEEE Journal of Emerging and Selected Topics in Power Electronics, vol. 4, no. 1, pp. 247–259 (2013), DOI: 10.1109/JESTPE.2013.2285376.

[19] Brayton R.K., Moser J.K., *A theory of nonlinear networks I, Quarterly of Applied Mathematics*, vol. 22, no. 1, pp. 1–33 (1964), DOI: 10.1090/qam/169746.

[20] Krishna Chaitanya K., Michele C., Jacquelien M.A.S., *Differentiation and Passivity for Control of Brayton–Moser Systems*, IEEE Transactions on Automatic Control, vol. 66, no. 3, pp. 1087–1101 (2021), DOI: 10.1109/TAC.2020.2994317.

[21] Kumari S., Rakesh M., Shambhu N.S., *Brayton–Moser passivity-based controller for electric vehicle battery charger*, CPSS Transactions on Power Electronics and Applications, vol. 6, no. 1, pp. 40–51 (2021), DOI: 10.24295/CPSSTPEA.2021.00004.

[22] Tomoaki H., *Implicit Model Predictive Control for Discretized Brayton–Moser Equations*, 2022 22nd International Conference on Control, Automation and Systems (ICCAS), no. 22510332 (2023), DOI: 10.23919/ICCAS55662.2022.10003788.

[23] Sonal G., Vivek P., Ragini M., *Brayton–Moser Modeling of Solid-State Transformer*, 2018 Condition Monitoring and Diagnosis (CMD), no. 18236333 (2018), DOI: 10.1109/CMD.2018.8535957.

[24] Shipra K., Maurya R., Sharma S.N., *Brayton–Moser passivity-based controller for electric vehicle battery charger*, CPSS Transactions on Power Electronics and Applications, vol. 6, no. 1, pp. 40–51 (2021), DOI: 10.24295/CPSSTPEA.2021.00004.

[25] Zhangjie L., Xin G., Mei S., *Complete Large-Signal Stability Analysis of DC Distribution Network via Brayton–Moser's Mixed Potential Theory*, IEEE Transactions on Smart Grid, vol. 14, no. 2, pp. 866–877 (2023), DOI: 10.1109/TSG.2022.3198496.

[26] Garcia Canseco E., Jeltsema D., Ortega R., *Power-based control of physical systems*, Automatica, vol. 46, no. 1, pp. 127–132 (2010), DOI: 10.1016/j.automatica.2009.10.012.